Multi-step shot noise spectrum induced by a local large spin*

Niu Peng-Bin(牛鹏斌)[a)†], Shi Yun-Long(石云龙)[a)], Sun Zhu(孙 祝)[a)], and Nie Yi-Hang(聂一行)[b)]

[a)] *Institute of Solid State Physics and Department of Physics, Shanxi Provincial Key Laboratory of Micro-structural Electromagnetic Functional Materials, Shanxi Datong University, Datong* 037009, *China*

[b)] *Institute of Theoretical Physics and Department of Physics, Shanxi University, Taiyuan* 030006, *China*

(Received 9 July 2015; revised manuscript received 15 August 2015; published online 20 October 2015)

We use non-equilibrium Green's function method to analyze the shot noise spectrum of artificial single molecular magnets (ASMM) model in the strong spin–orbit coupling limit in sequential tunneling regime, mainly focusing on the effects of local large spin. In the linear response regime, the shot noise shows $2S+1$ peaks and is strongly spin-dependent. In the nonlinear response regime, one can observe $2S+1$ steps in shot noise and Fano factor. In these steps one can see the significant enhancement effect due to the spin-dependent multi-channel process of local large spin, which reduces electron correlations.

Keywords: artificial single molecular magnet, Hubbard operator Green's function, shot noise

PACS: 73.63.Kv, 72.70.+m, 73.23.Hk, 73.63.–b **DOI:** 10.1088/1674-1056/24/12/127309

1. Introduction

Single molecular magnets (SMMs), characterized by a local large spin and magnetic anisotropy, have attracted much attention in the last two decades for showing the macroscopic quantum coherence[1–4] and macroscopic quantum tunneling.[5–10] Since Heersche *et al.*[11] were able to trap an SMM in a typical field transistor geometry, great efforts have been devoted to measuring electronic transport through an SMM, which has a potential application for magnetic devices and quantum computation.[12]

Although theoretical and experimental studies have revealed a lot of fascinating transport properties, such as negative differential conductance,[11,13–16] current-induced switching,[17–20] Kondo effect,[21–29] Berry phase blockade,[2] and thermoelectric effect,[30,31] it is still very challenging in experiments to control such molecules. So it is natural to consider artificial counterparts of SMM, just like quantum dots as artificial counterparts of an atom. In Refs. [32] and [33], it was suggested that one can study an alternative, i.e., Mn-doped quantum dots, which behave as SMMs and are called artificial single molecular magnets (ASMMs). In Ref. [32] it was proved that Mn-doped quantum dots indeed behave like a nanomagnet with hysteretic magnetization and steps of the magnetization. In Ref. [33] they studied the shot noise spectrum by using quantum master equation method and found a distinct effect similar to the Dicke effect in quantum optics.

In this paper we use non-equilibrium Green's function method to consider the shot noise spectrum of ASMM model in the strong spin–orbit coupling limit in sequential tunneling regime, mainly focusing on the effects of local large spin in the low and high temperatures. To deal with the local large spin, we use the language of molecular states, i.e., the Hubbard operators.[34–36] In the linear response regime, the shot noise shows $2S+1$ peaks and is strongly spin-dependent. In the nonlinear response regime, one can observe $2S+1$ steps in shot noise spectrum and Fano factor. In these steps one can see the significant enhancement effect due to the spin-dependent multi-channel process which reduces electron correlations.

This paper is organized as follows. In Section 2 we describe the model of artificial single molecular magnets and Hubbard operator Green's function method. Specific Hamiltonian, basic formula for non-equilibrium Green's functions are presented there. In Section 3 we present the numerical results and explain the $2S+1$ step structure induced by the spin-dependent multi-channel process. Finally, Section 4 is devoted to a brief conclusion.

2. Model and non-equilibrium Green's function method

In this work, we adopt the model proposed by Pulido *et al.*[32,33] For simplicity, we consider the minimal model with only z axis electron–Mn exchange interaction in the strong spin–orbit coupling. The total Hamiltonian of the system can be written as $H = H_{\rm leads} + H_T + H_{\rm cen}$:

$$H_{\rm leads} = \sum_{k\alpha\sigma} \varepsilon_{k\alpha} c^{\dagger}_{k\alpha\sigma} c_{k\alpha\sigma}, \tag{1}$$

$$H_{\rm T} = \sum_{k\alpha\sigma} (t_{k\alpha} c^{\dagger}_{\sigma} c_{k\alpha\sigma} + {\rm H.c.}), \tag{2}$$

$$H_{\rm cen} = \varepsilon_0 (n_{\uparrow} + n_{\downarrow}) + U n_{\uparrow} n_{\downarrow} + J s_z S_z, \tag{3}$$

where $\varepsilon_{k\alpha}$ is the energy for free electrons, with $\alpha = L, R$ enumerating left and right leads, and $c^{\dagger}_{k\alpha\sigma}(c_{k\alpha\sigma})$ are elec-

*Project supported by the National Natural Science Foundation of China (Grant Nos. 11504210, 11504211, 11504212, 11274207, 11274208, 11174115, and 11325417), the Key Program of the Ministry of Education of China (Grant No. 212018), the Scientific and Technological Project of Shanxi Province, China (Grant No. 2015031002-2), the Natural Science Foundation of Shanxi Province, China (Grant Nos. 2013011007-2 and 2013021010-5), and the Outstanding Innovative Teams of Higher Learning Institutions of Shanxi Province, China.

†Corresponding author. E-mail: niupengbin@163.com

© 2015 Chinese Physical Society and IOP Publishing Ltd

tronic creation (annihilation) operators in the electrodes, with $\sigma = \uparrow, \downarrow$ representing the electron spin-up and spin-down. $t_{k\alpha}$ are the tunneling amplitudes. ε_0 is the single level energy of the quantum dot imbedded in the transport, and U is Coulomb interaction strength, with $\hat{n}_\sigma = c_\sigma^\dagger c_\sigma$ the number operator. The $c_\sigma^\dagger$ and c_σ are electronic creation and annihilation operators on the single level of the dot. S^z is the z component of the local spin and $s^z = (n_\uparrow - n_\downarrow)/2$ is the spin of the electron on the dot. The corresponding operators $S^\pm$ ($s^\pm$) are the ladder operators. According to Ref. [33], this model can be realized in a CdTe quantum dot doped with a single Mn^{+2} ion with spin $S = 5/2$. In their original model, they consider the exchange interaction

$$H_{\text{exch}} = Js_zS_z + \frac{1}{2}\alpha J(s_+S_- + s_-S_+),$$

where α can be equal to zero due to strong spin–orbit coupling. This system behaves as an SMM with magnetization steps and hysteresis. Its shot noise spectrum depends on the quantum state of the Mn spin, which can be seen clearly in the following main text.

The eigenstates and energies for the isolated Hamiltonian H_{cen} in Eq. (3) are easily obtained as

$$\begin{aligned} H_{\text{cen}}|0m\rangle &= 0\,|0m\rangle\,, \\ H_{\text{cen}}|\uparrow m\rangle &= \left(\varepsilon_0 + \frac{J}{2}m\right)|\uparrow m\rangle\,, \\ H_{\text{cen}}|\downarrow m\rangle &= \left(\varepsilon_0 - \frac{J}{2}m\right)|\downarrow m\rangle\,, \end{aligned} \tag{4}$$

where eigenstates $\{|0m\rangle\}$ with energy $E = 0$ are for $n = 0$ electron sector and eigenstates $\{|\uparrow m\rangle, |\downarrow m\rangle\}$ with energy $E = \varepsilon_0 \pm \frac{J}{2}m$ are for $n = 1$ electron sector, respectively. Notice that for simplicity we do not consider a double-occupation sector in this work.

The non-equilibrium Green's function (GF) approach in the language of molecular states, i.e., the language of Hubbard operators is used in this paper.[34–41] This method absorbs the advantage of quantum master equations, which use many-body states as the basis in the reduced density matrix.[42] In this Hubbard operator representation, the electron operators in the dot are rewritten as $c_\sigma = X^{0\sigma} + \delta_\sigma X^{\bar{\sigma}2}$ with $\delta_\sigma = +1$ (-1) for $\sigma = \uparrow$ $(\downarrow)$, $s^z = \frac{1}{2}\left(X^{\uparrow\uparrow} - X^{\downarrow\downarrow}\right)$, $s^+ = X^{\uparrow\downarrow}$ and $s^- = X^{\downarrow\uparrow}$. In one-electron regime $(U \to \infty)$ the double-occupation is forbidden and $c_\sigma = X^{0\sigma}$. The large spin operators can be expressed as[34–36] $S^z = \sum_{m=-S}^{S} mY^{mm}$, $S^+ = \sum_{m=-S}^{S} C_m^+ Y^{m+1,m}$, and $S^- = \sum_{m=-S}^{S} C_m^- Y^{m-1,m}$, where S is the large spin quantum number and $Y^{m,n} = |Sm\rangle\langle Sn|$. Then the equation of motion (EOM) procedure can be applied as usual.[43,44] The second-order truncation for the Green's functions is used to capture sequential tunneling physics.[45] In the presence of large Coulomb interaction energy, we consider only states with $n = 0, 1$ electrons, which simplify the calculation a lot in sequential tunneling regime. The retarded Green's function is expressed as

$$G_\sigma^{\text{r}}(\omega) = \sum_{m=-S}^{S} \frac{P_{0m} + P_{\sigma m}}{\omega - \varepsilon_0 - \delta_\sigma \frac{J}{2}m - \Sigma_0}, \tag{5}$$

with the self-energy $\Sigma_0 = \sum_{k\alpha} |t_{k\alpha}|^2 / (\omega - \varepsilon_{k\alpha} + \mathrm{i}0^+)) = -\mathrm{i}\Gamma_{\text{L}}$ and $P_{\lambda m} \equiv \langle X^{\lambda\lambda} Y^{mm} \rangle$. For technical details, one can refer to our previous papers.[34–36]

Once the single-particle Green's function is obtained, the occupation, current, shot noise, and Fano factor can be calculated along the lines of Refs. [46] and [47]. The transport current is

$$I = -\frac{e}{h}\frac{\Gamma_{\text{L}} + \Gamma_{\text{R}}}{\Gamma_{\text{L}}\Gamma_{\text{R}}} \sum_\sigma \int \mathrm{d}\omega (f_{\text{L}} - f_{\text{R}}) \mathrm{Im} G_\sigma^{\text{r}}(\omega). \tag{6}$$

The zero-frequency current noise is

$$\begin{aligned} S(0) = &-\frac{e^2}{h}\frac{\Gamma_{\text{L}} + \Gamma_{\text{R}}}{\Gamma_{\text{L}}\Gamma_{\text{R}}} \sum_\sigma \int \mathrm{d}\omega \{[f_{\text{L}}(1 - f_{\text{L}}) \\ &+ f_{\text{R}}(1 - f_{\text{R}})] \mathrm{Im} G_\sigma^{\text{r}}(\omega) \\ &+ (f_{\text{L}} - f_{\text{R}})^2 \mathrm{Im} G_\sigma^{\text{r}}(\omega)(1 + \Gamma_{\text{L}} \mathrm{Im} G_\sigma^{\text{r}}(\omega))\}. \end{aligned} \tag{7}$$

In Eqs. (6) and (7) $f_{\text{L/R}}(\omega) = \left[\mathrm{e}^{\beta(\omega - \mu_{\text{L/R}})} + 1\right]^{-1}$ is the Fermi–Dirac distribution function with $\beta = 1/k_{\text{B}}T$.

3. Results and discussion

In this section we present the transport results of occupation of states, local spin projection, shot noise, and Fano factor in linear and nonlinear response regimes.

3.1. Shot noise spectrum in linear-response regime

In this subsection we focus on the transport properties of occupation of states, local spin projection, shot noise, and Fano factor in the linear response regime. Before numerical discussion, we briefly show here that the fluctuation–dissipation theorem $S(0) = 4G_{\text{dc}}(0)/\beta$, which relates Nyquist–Johnson noise with the linear conductance, can be obtained in the language of GF: In the limit $V \to 0$, the linear conductance obtained from Eq. (6) reads

$$G_{\text{dc}}(0) = -\frac{1}{\pi}\Gamma_{\text{L}} \int \mathrm{d}\omega [\beta\, \mathrm{e}^{\beta\omega}/(\mathrm{e}^{\beta\omega} + 1)^2] \mathrm{Im} G_\uparrow^{\text{r}}(\omega),$$

where we have used that $\Gamma_{\text{L}} = \Gamma_{\text{R}}$, and in Eq. (7) the first term is the equilibrium noise contribution and the second term is the non-equilibrium contribution, which vanish when $V \to 0$, so equilibrium noise

$$S(0) = -\frac{4}{\pi}\Gamma_{\text{L}} \int \mathrm{d}\omega [\beta\, \mathrm{e}^{\beta\omega}/(\mathrm{e}^{\beta\omega} + 1)^2] \mathrm{Im} G_\uparrow^{\text{r}}(\omega)$$

is obtained. One can see here the fluctuation–dissipation theorem is recovered.

As a simple and clear start, we discuss $S = 1/2$ case first and then compare it with $S = 5/2$. The eigenstates and energies for $S = 1/2$ reads

$$N = 0 : H_{\text{cen}} \left|0, \pm\tfrac{1}{2}\right\rangle = 0 \left|0, \pm\tfrac{1}{2}\right\rangle;$$

$$
\begin{aligned}
&N=1,\mathrm{FM}:\\
&\quad\begin{cases} H_{\mathrm{cen}}\left|\uparrow,\frac{1}{2}\right\rangle=\left(\varepsilon_0+\frac{J}{4}\right)\left|\uparrow,\frac{1}{2}\right\rangle,\\ H_{\mathrm{cen}}\left|\downarrow,-\frac{1}{2}\right\rangle=\left(\varepsilon_0+\frac{J}{4}\right)\left|\downarrow,-\frac{1}{2}\right\rangle;\end{cases}\\
&N=1,\mathrm{AF}:\\
&\quad\begin{cases} H_{\mathrm{cen}}\left|\uparrow,-\frac{1}{2}\right\rangle=\left(\varepsilon_0-\frac{J}{4}\right)\left|\uparrow,-\frac{1}{2}\right\rangle,\\ H_{\mathrm{cen}}\left|\downarrow,\frac{1}{2}\right\rangle=\left(\varepsilon_0-\frac{J}{4}\right)\left|\downarrow,\frac{1}{2}\right\rangle.\end{cases}
\end{aligned}
\tag{8}
$$

There are three branches of states: the empty ($N=0$) sector and the two singly-occupied ($N=1$) sectors which include the ferromagnetic (FM) sector and the anti-ferromagnetic (AF) sector.

In Fig. 1 we present the occupation of states, local spin projection, and linear shot noise for $S=1/2$ case as a function of gate voltage. The average values of state occupation $P_0\equiv P_{0m}$ and $P_{\uparrow m}$ are defined as $\langle|0,m\rangle\langle 0,m|\rangle$ and $\langle|\uparrow,m\rangle\langle\uparrow,m|\rangle$. They can be explained as density matrix elements in the language of master equation and will be calculated via Green's functions in this paper. Their values are strongly affected by the environment such as gate voltage or bias voltage when non-equilibrium transport sets in. In numerical calculation we have used the properties that $P_{0m}=P_{0m'}$ and $P_{\uparrow m}=P_{\downarrow -m}$, which comes from the symmetry of the Hamiltonian. The average value of local spin projection are defined as $L_m\equiv\langle|Sm\rangle\langle Sm|\rangle$. Now we are ready to discuss them. In the region $V_{\mathrm{g}}>0.1$, $|0,\pm 1/2\rangle$ occupy, i.e., $P_{0\frac{1}{2}}=P_{0-\frac{1}{2}}=1/2$, so there is no electron on the ASMM. When decreasing the gate voltage, the first charge degeneracy point between $|0,-1/2\rangle$ and AF state $|\uparrow,-1/2\rangle$ (or $|0,1/2\rangle$ and $|\downarrow,1/2\rangle$) at $V_{\mathrm{g}}=0.1$ is reached, and shot noise exhibits a peak in Fig. 1(c). In the region between $0.1V_{\mathrm{g}}$ and $-0.1V_{\mathrm{g}}$, $P_{\uparrow-\frac{1}{2}}=P_{\downarrow\frac{1}{2}}=0.5$, i.e., AF states $|\uparrow,-1/2\rangle$ and $|\downarrow,1/2\rangle$ occupy and the occupation of states $|0,\pm 1/2\rangle$ becomes zero. At $V_{\mathrm{g}}=-0.1$, the second charge degeneracy point between $|0,\pm 1/2\rangle$ and the FM branch is reached, and a small peak in shot noise in Fig. 1(c) shows. This can be understood as follows: we assume single electron occupation is allowed and most of the probability is occupied by an electron on AF state which is saturated below the Fermi surface first and only a little probability is allowed for the FM branch to occupy due to higher order co-tunneling process, which causes the lowest lying electron to jump out. The same argument applies to $S=5/2$ case, and there will only be a main peak and five small peaks, which become smaller and smaller when decreasing gate voltage [see Fig. 2(c)]. In the region below $-0.1V_{\mathrm{g}}$, the FM branch is also below the Fermi surface, and begins to compete with the AF branch, so each occupation of AF/FM is smaller than $1/2$, and in the situation when V_{g} is small enough, i.e., both AF and FM are far from the Fermi surface, AF and FM will be occupied equally, $P_{\uparrow-\frac{1}{2}}=P_{\downarrow\frac{1}{2}}=P_{\uparrow\frac{1}{2}}=P_{\downarrow-\frac{1}{2}}=1/4$, and the red and blue lines in Fig. 1(a) will meet each other eventually.

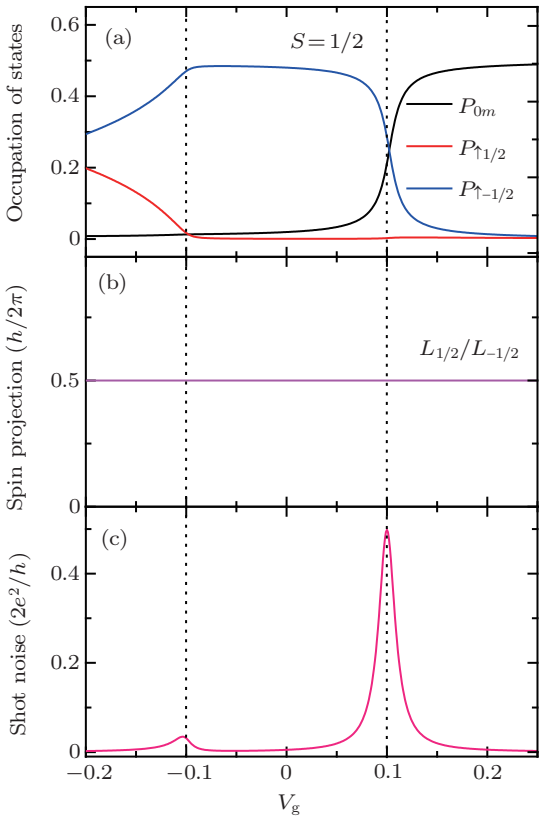


Fig. 1. (color online) $S=1/2$ case. Occupation of states (a) and local spin projection (b), as well as linear shot noise (c), calculated as a function of the gate voltage. The parameters are chosen as $J=0.4$, $\Gamma_{\mathrm{L}}=0.01$, and zero temperature. Energy unit is given in the half-bandwidth D.

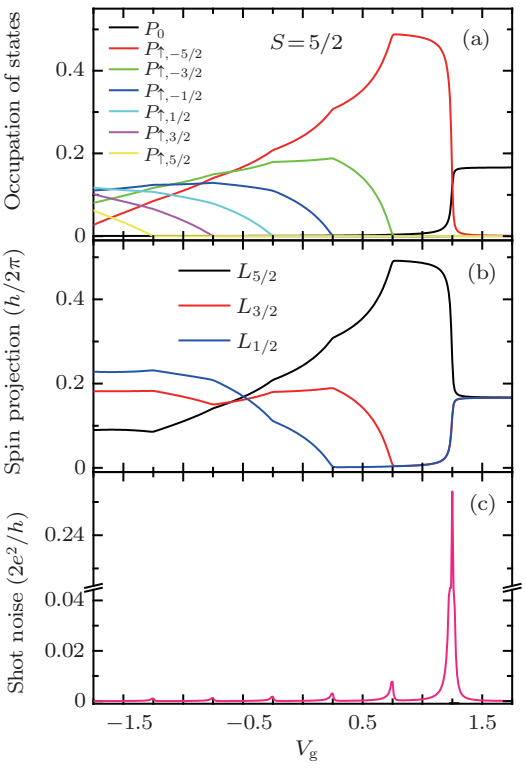


Fig. 2. (color online) $S=5/2$ case. Occupation of states (a) and local spin projection (b), as well as linear shot noise (c), calculated as a function of the gate voltage for the parameters: $J=0.4$, $\Gamma_{\mathrm{L}}=0.01$, and zero temperature. Energy unit is given in the half-bandwidth D.

Let us now discuss the $S = 5/2$ case. In Fig. 2(a) when $V_g > 1.25$, P_0 dominates and $P_0 = 1/6$. Decreasing gate voltage to $1.25V_g$, the first charge degeneracy point is reached and induces the main peak in Fig. 2(c). In the region between $1.25V_g$ and $0.75V_g$, $P_{\uparrow-\frac{5}{2}}/P_{\downarrow\frac{5}{2}}$ occupy and $P_{\uparrow-\frac{5}{2}} = P_{\downarrow\frac{5}{2}} = 0.5$. When $V_g = 0.75$, the second charge degeneracy point is reached. In the region between $0.75V_g$ and $0.25V_g$, $P_{\uparrow-\frac{3}{2}}/P_{\downarrow\frac{3}{2}}$ sets in and competes with $P_{\uparrow-5/2}/P_{\downarrow\frac{5}{2}}$, and in Fig. 2(a) the blue line begins to increase and the red line begins to decrease. The same analysis continues when sweeping down the gate voltage. Here we want to stress the difference of local spin projection between $S = 1/2$ and $S = 5/2$ [see Fig. 1(b) and Fig. 2(b)]. Although $\langle S_z\rangle = 0$ for $\langle S_z\rangle = \sum_m mL_m$ and $L_m = L_{-m}$, L_m vary with V_g and they are spin-dependent. First let us take a glance from the formula $L_m = P_0 + P_{\uparrow m} + P_{\downarrow m}$. For $S = 1/2$, $L_{\frac{1}{2}} = P_0 + P_{\uparrow\frac{1}{2}} + P_{\downarrow\frac{1}{2}} = P_0 + P_{\uparrow-\frac{1}{2}} + P_{\downarrow-\frac{1}{2}} = 1/2$, so it is not spin-dependent, i.e., irrelevant to spin-up or spin-down. But for $S = 5/2$ and taking $L_{-\frac{5}{2}} = P_0 + P_{\uparrow-\frac{5}{2}} + P_{\downarrow-\frac{5}{2}}$ for example, $L_{-\frac{5}{2}} \neq L_{-\frac{3}{2}} \neq L_{-\frac{1}{2}}$ and is strongly affected by the competition between each $|Sm\rangle$ branch when varying V_g.

3.2. Shot noise spectrum in nonlinear-response regime

In this subsection we will focus on the transport in the nonlinear-response regime. In Fig. 3 we plot the non-equilibrium shot noise and Fano factor ($F = S/2eI$) as a function of bias voltage for $S = 5/2$ in the low temperature. In Fig. 3(a) one can observe $2S+1$ steps in the shot noise spectrum and correspondingly in Fig. 3(b) there are $2S+1$ steps in the Fano factor. In the non-equilibrium regime, and for temperature $T \to 0$, the equilibrium noise contribution vanishes, and the noise in Eq. (7) reduces to

$$S = -\frac{2}{\pi}\Gamma_L \int_0^V d\omega \mathrm{Im}G^r_\uparrow(\omega)[1 + \Gamma_L \mathrm{Im}G^r_\uparrow(\omega)]. \qquad (9)$$

The shot noise steps observed in Fig. 3(a) can be better understood by analyzing the current. Increasing V one observes that the current is suppressed until the lowest AF states are reached. As the bias voltage increases further, shot noise is enhanced every time the current is allowed, defining the steps structure. In Fig. 3(b) for $V < 0.75$, the Fano factor is unity, which indicates the first-order sequential tunneling processes are suppressed and the transport occurs due to second-order elastic co-tunneling processes. Such processes are stochastic and uncorrelated in time, so the shot noise is Poissonian. Above the 0.75 voltage, sequential tunneling processes dominate transport and the noise becomes sub-Poissonian, which indicates that that tunneling processes in the sequential tunneling regime are correlated due to Coulomb correlation and Pauli principle. For $V > \varepsilon_0 - \frac{5}{4}J$, we can see the significant enhancement of the Fano factor due to the multi-channel process which reduces electron correlations compared to the single-channel model [Fig. 3(b) inset].

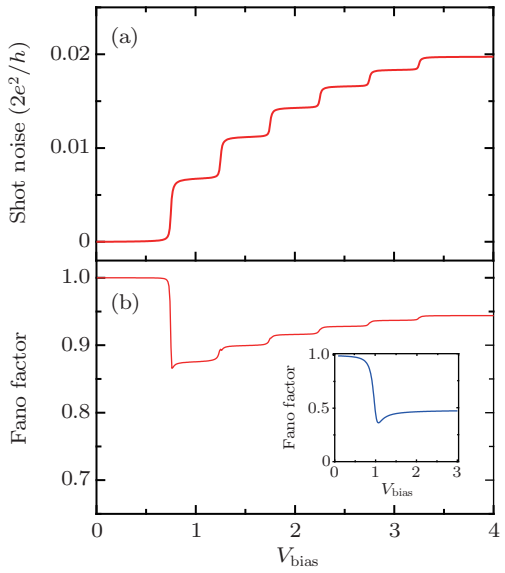


Fig. 3. (color online) Non-equilibrium shot noise (a), as well as Fano factor (b), calculated as a function of the bias voltage for $S = 5/2$. Parameters: $\varepsilon_0 = 2, J = 1, \Gamma_L = \Gamma_R = 0.01$, and zero temperature. Inset: Fano factor for single-channel model with parameters $\varepsilon_0 = 1$ and $\Gamma_L = \Gamma_R = 0.1$. Energy unit is given in the half-bandwidth D.

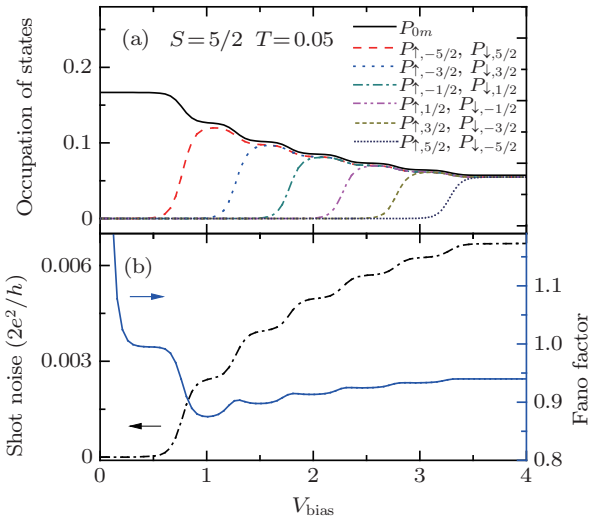


Fig. 4. (color online) Occupation of states (a), and shot noise, and Fano factor (b) as a function of the bias voltage for $S = 5/2$. Parameters are the same as those in Fig. 3 with $T = 0.05$.

Let us now discuss the high temperature situation. In Fig. 4 we plot the non-equilibrium occupation of states, shot noise, and Fano factor as a function of bias voltage for $S = 5/2$. We first discuss the occupations in Fig. 4(a). For $V < 0.75$, zero occupancy dominates and $P_{0m} = 1/6$. Increasing the bias voltage the lowest AF states $|\uparrow, -5/2\rangle$ and $|\downarrow, 5/2\rangle$ enter the bias window and share the occupation probability with $n = 0$ states and $P_0 = P_{\uparrow-5/2} = 1/8$. When we further increase V,

other states come into the bias window one-by-one and figure 4(a) exhibits the step structures. The Fano factor as a function of the bias voltage is shown in Fig. 4(b). For the low bias voltage ($V < 0.25$), the shot noise is determined by thermal Johnson–Nyquist noise which results in a divergency of the Fano factor for $V \to 0$. One can also observe $2S+1$ steps in shot noise and Fano factor in the high temperature situation, but these steps are less clear due to the temperature effect.

4. Conclusion

In conclusion, we have used non-equilibrium Green's function method to analyze the shot noise spectrum of artificial single molecular magnets (ASMM) model in the strong spin–orbit coupling limit in the sequential tunneling regime, mainly focusing on the effects of local large spin in the low and high temperatures. In the linear response regime, the shot noise shows $2S+1$ peaks and is strongly spin-dependent. In the nonlinear response regime, one can observe $2S+1$ steps in the shot noise spectrum and Fano factor. In these steps one can see the significant enhancement effect due to the spin-dependent multi-channel process which reduces electron correlations.

References

[1] Wernsdorfer W and Sessoli R 1999 *Science* **284** 133
[2] González G and Leuenberger M N 2007 *Phys. Rev. Lett.* **98** 256804
[3] González G, Leuenberger M N and Mucciolo E R 2008 *Phys. Rev. B* **78** 054445
[4] Gunther L and Barbara B 1994 *Quantum Tunneling of Magnetization* (Dordrecht: Kluwer)
[5] Leggett A J, Chakravarty S, Dorsey A T, Fisher M P A, Garg A and Zwerger W 1987 *Rev. Mod. Phys.* **59** 1
[6] Loss D, Divincenzo D P and Grinstein G 1992 *Phys. Rev. Lett.* **69** 3232
[7] Delft J V and Henley C L 1992 *Phys. Rev. Lett.* **69** 3236
[8] He G, He L H, Zhang J R, Cao H B, Yan L Q, Wang F W and Yan Q W 2007 *Chin. Phys.* **16** 1776
[9] Zhang S Q and Chen Z D 2008 *Chin. Phys. B* **17** 1436
[10] Zhang S Q and Chen Z D 2008 *Commun. Theor. Phys.* **50** 248
[11] Heersche H B, de Groot Z, Folk J A, van der Zant H S J, Romeike C, Wegewijs M R, Zobbi L, Barreca D, Tondello E and Cornia A 2006 *Phys. Rev. Lett.* **96** 206801
[12] Hou J M, Tian L J and Ge M L 2005 *Chin. Phys. Lett.* **22** 2147
[13] Elste F and Timm C 2006 *Phys. Rev. B* **73** 235305
[14] Timm C and Elste F 2006 *Phys. Rev. B* **73** 235304
[15] Luo W, Wang R Q, Hu L B and Yang M 2013 *Chin. Phys. B* **22** 047201
[16] Chang B and Liang J Q 2011 *Chin. Phys. B* **20** 017307
[17] Misiorny M and Barnas J 2007 *Phys. Rev. B* **75** 134425
[18] Misiorny M and Barnas J 2007 *Phys. Rev. B* **76** 054448
[19] Misiorny M and Barnas J 2008 *Phys. Rev. B* **77** 172414
[20] Zhang Z Z, Shen R, Sheng L, Wang R Q, Wang B G and Xing D Y 2011 *Chin. Phys. B* **20** 047504
[21] Romeike C, Wegewijs M R, Hofstetter W and Schoeller H 2006 *Phys. Rev. Lett.* **96** 196601
[22] Romeike C, Wegewijs M R, Hofstetter W and Schoeller H 2006 *Phys. Rev. Lett.* **97** 206601
[23] Leuenberger M N and Mucciolo E R 2006 *Phys. Rev. Lett.* **97** 126601
[24] Zitko R, Peters R and Pruschke Th 2008 *Phys. Rev. B* **78** 224404
[25] Hackl A, Roosen D, Kehrein S and Hofstetter W 2009 *Phys. Rev. Lett.* **102** 196601
[26] Misiorny M, Weymann I and Barnas J 2011 *Phys. Rev. Lett.* **106** 126602
[27] Elste F and Timm C 2010 *Phys. Rev. B* **81** 024421
[28] Wang R Q and Jiang K M 2009 *Chin. Phys. B* **18** 5443
[29] Wang R Q and Jiang K M 2010 *Commun. Theor. Phys.* **53** 370
[30] Wang R Q, Sheng L, Shen R, Wang B and Xing D Y 2010 *Phys. Rev. Lett.* **105** 057202
[31] Misiorny M and Barnas J 2015 *Phys. Rev. B* **91** 155426
[32] Fernandez-Rossier J and Aguado R 2006 *Phys. Stat. Sol.* **3** 3734
[33] Contreras-Pulido L D and Aguado R 2010 *Phys. Rev. B* **81** 161309
[34] Niu P B, Zhang Y Y, Wang Q and Nie Y H 2012 *Phys. Lett. A* **376** 1481
[35] Niu P B, Yao H, Li Z J and Nie Y H 2012 *J. Magn. Magn. Mater.* **324** 2324
[36] Niu P B, Wang Q and Nie Y H 2013 *Chin. Phys. B* **22** 027307
[37] Jonas Fransson 2010 *Non-Equilibrium Nano-Physics: A Many-Body Approach* (Dordrecht: Springer)
[38] Fransson J, Eriksson O and Sandalov I 2002 *Phys. Rev. Lett.* **88** 226601
[39] Kostyrko T and Bułka B R 2005 *Phys. Rev. B* **71** 235306
[40] Esposito M and Galperin M 2009 *Phys. Rev. B* **79** 205303
[41] Yang M, Ran X J, Cui Y and Wang R Q 2011 *Chin. Phys. B* **20** 097201
[42] Timm C and Elste F 2006 *Phys. Rev. B* **73** 235304
[43] Meir Y, Wingreen N S and Lee P A 1993 *Phys. Rev. Lett.* **70** 2601
[44] Haug H and Jauho A P *Quantum Kinetics in Transport and Optics of Semiconductors* (Berlin: Springer)
[45] Tolea M and Bułka B R 2007 *Phys. Rev. B* **75** 125301
[46] Meir Y and Wingreen N S 1992 *Phys. Rev. Lett.* **68** 2512
[47] Zhu J X and Balatsky A V 2003 *Phys. Rev. B* **67** 165326